BBA - Molecular Basis of Disease 1870 (2024) 166873

Contents lists available at ScienceDirect

BBA - Molecular Basis of Disease

journal homepage: www.elsevier.com/locate/bbadis

FTIR Microspectroscopy as a new probe to study human uterine lesions: Characterization of tumor cell lines from uterine smooth muscle cells and evaluation of EPA and DHA *in vitro* treatments

Alessia Belloni [a,1], Valentina Notarstefano [a,1], Stefania Greco [b,1], Pamela Pellegrino [b], Elisabetta Giorgini [a,*], Pasquapina Ciarmela [b]

[a] Department of Life and Environmental Sciences, Università Politecnica delle Marche, Ancona, Italy
[b] Department of Experimental and Clinical Medicine, Università Politecnica delle Marche, Ancona, Italy

ARTICLE INFO

Keywords:
Uterine leiomyoma
Uterine leiomyosarcoma
Fourier Transform InfraRed Microscopy (FTIRM)
Omega-3 fatty acids
Eicosapentaenoic acid (EPA)
Docosahexaenoic acid (DHA)

ABSTRACT

During their life, women are likely to develop uterine diseases, which often compromise their fertile and perimenopausal age. Besides benign lesions like leiomyomas, several malignant neoplasms can occur, such as the uterine leiomyosarcoma, which represents the most frequent malignancy among the rarest uterine cancers. It presents several variants similar to both benign and malignant neoplasms, and sometimes it shares symptoms with the benign counterpart. In this scenario, for a correct diagnosis and a successful prognosis, it is mandatory to detect new reliable markers which strengthen histopathological outcomes and let define a more appropriate and less harmful therapy. Based on this concerning evidence, in the present study, Fourier Transform Infrared Microspectroscopy has been exploited at a cellular level on uterine leiomyoma and leiomyosarcoma cell lines to (1) identify specific spectral biomarkers able to distinguish between benign and malignant lesions, and (2) evaluate the efficacy of eicosapentaenoic and docosahexaenoic acids (respectively EPA and DHA), already successfully tested. Results evidenced reliable differences in the spectral signature of benign and malignant cells, mainly in terms of lipids and nucleic acids composition. Moreover, even if EPA and DHA seemed to exert different effects on the tested cell lines, no cytotoxic and/or anti-apoptotic actions were observed after omega-3 based treatments.

1. Introduction

Gynecologic diseases include several kinds of benign and malignant tumor lesions, which affect the endometrial compartment, cervix, ovaries, vulva, and vagina. All these pathologies may arise during both fertile or perimenopausal age and can occur with common symptoms such as abnormal uterine bleeding, abdominal or pelvic discomfort, and so on [1,2]. To date, besides the decreasing trend registered in the last years, gynecologic diseases still show high incidence and death rates, and surgical rescission or hysterectomy represent the treatments of choice in addition to hormonal therapy, chemotherapy, and radiotherapy [3–5].

Uterine leiomyoma (uLM) and uterine leiomyosarcoma (uLMS) are two monoclonal mesenchymal tumor lesions spreading inside the uterine cavity from uterine myometrial smooth muscle cells; they share common symptoms and morphological features, even if they are respectively a benign and a malignant lesion with totally different clinical outcomes and incidence rates [6]. This evidence can make difficult a correct diagnosis, mainly in the early developmental stages. It is noteworthy that imaging techniques routinely used in these cases are not always sufficient to distinguish between benign and malignant lesions, and hence the post-operative diagnosis remains the only choice, even if it causes a delay in starting the appropriate therapy [7–10]. In addition, even after surgery, the diagnosis may be further complicated by the existence of several other subvariants. In fact, leiomyoma and leiomyosarcoma represent the two endpoints of several other uterine neoplasms not yet well classified, including lesions with benign and/or malignant potential, currently known as “atypical” or generally variants

* Corresponding author.
E-mail addresses: a.belloni@univpm.it (A. Belloni), v.notarstefano@univpm.it (V. Notarstefano), s.greco@univpm.it (S. Greco), p.pellegrino@pm.univpm.it (P. Pellegrino), e.giorgini@univpm.it (E. Giorgini), p.ciarmela@univpm.it (P. Ciarmela).
[1] These authors equally contributed as first authors.

https://doi.org/10.1016/j.bbadis.2023.166873
Received 30 May 2023; Received in revised form 5 August 2023; Accepted 31 August 2023
Available online 2 September 2023

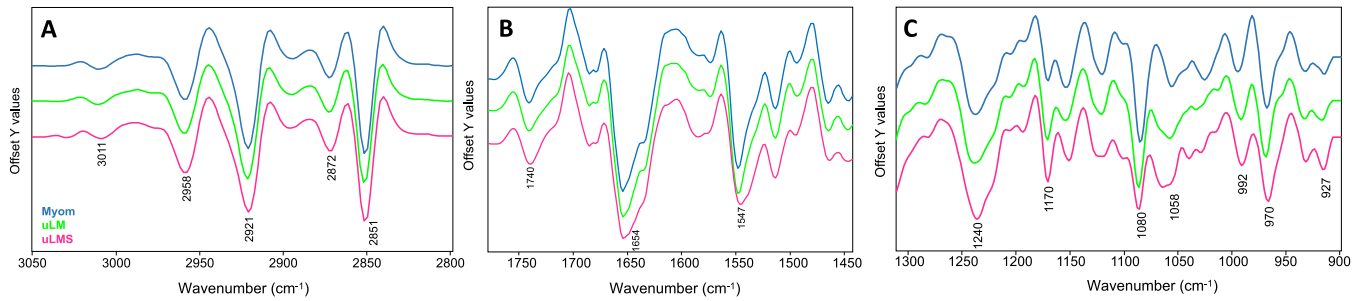

Fig. 1. Second derivative average spectra of myometrium (Myom; blue line), leiomyoma (uLM; green line), and leiomyosarcoma (uLMS; red line) cell lines in the following spectral ranges: (A) 3050–2800 $cm^{-1,}$ related to lipids; (B) 1780–1480 cm^{-1}, related to proteins, and (C)1310–900 cm^{-1}, related to nucleic acids and carbohydrates. Spectra are off set along y-axis for a better comprehension.

Table 1
Meaningful IR bands (reported as wavenumbers) identified in the IR spectra of myometrium (Myom), leiomyoma (uLM), and leiomyosarcoma (uLMS) cell lines and corresponding biochemical assignments.

Wavenumbers (cm^{-1})	Assignment
~3014	Stretching of =C-H moiety in lipids [36,37]
~2959	Asymmetric stretching of CH_3 moieties in branched aliphatic lipid chains [31,32]
~2923	Asymmetric stretching of CH_2 moieties in linear aliphatic lipid chains [38]
~1740	Stretching of C═O ester groups in lipids [38,39]
~1652 and ~1542	Vibrational modes of the peptide linkage, Amide I and II bands of proteins [28,40]
~1172	Stretching of C-OP moiety in non-hydrogen bonds groups [41,42]
~1080	Symmetric stretching of PO_2^- groups in nucleic acids [43]
~1058	Stretching of C-OH bond in oligosaccharides [40,44]
~992	Vibrational modes of RNA [40,45]
~965	Vibrational modes of DNA backbone [44,46,47]
~927	Vibrational modes of left-handed helix DNA (Z form) [31]

[11]. The so-called STUMP, uterine smooth muscle tumors of uncertain malignant potential, includes a heterogeneous group of lesions defined by histopathological criteria which partially match with features belonging to the benign counterpart promoted by leiomyoma or with ones belonging to the malignant represented by leiomyosarcoma [12–14].

Another relevant scientific concern is related to the need of innovative therapeutic approaches, less invasive as regards side effects and more efficient in reducing not only the symptoms but also the tumor progression. Besides the hormonal and chemotherapy treatments routinely used for leiomyoma and leiomyosarcoma, which have positive but also negative side effects, in recent years, much attention has been paid to long-chain omega-3 polyunsaturated fatty acids (PUFAs), and to their beneficial effects in human health, which include the modulation of lipid signaling and inflammation also in several women-affecting diseases [15–18]. Among the most known, the eicosapentaenoic (EPA) and docosahexaenoic (DHA) acids can be administered as supplements or taken through the diet with the consumption of seafood products, green leaves vegetables, nuts, and seeds [19,20]. Recent results demonstrated that EPA and DHA can sustain the psychomotor neurodevelopment in the first months of life, reduce oxidative stress and inflammation in women over the menstrual cycle, up to improve patients' conditions in autoimmune, inflammatory, cardiovascular, and neurological diseases [21–25]. These omega-3 unsaturated fatty acids seem to play a key role also in tumoral lesions. In fact, they do not only counteract chemo/radiotherapy consequences in oncological patients, but also suppress the progression of the tumor disease and inhibit inflammation and angiogenesis, two main cancer-related signals. Previous studies pinpointed also the efficacy of EPA and DHA in reducing collagen over-production in uterine leiomyoma [26–28]. EPA has already demonstrated its ability to impair collagen reorganization also in the wound-healing repairing process, impacting the quality of the wound tissue [29]. On the other hand, DHA was tested in several tumor kinds, displaying anti-inflammatory, antiproliferative, proapoptotic, antiangiogenic, anti-invasive, and antimetastatic properties [17,18,23].

Usually, the most known techniques used for cellular analyses, like PCR, flow cytometry, or the immunocytochemistry and immunohistochemistry are able to collect important and specific information but often as expensive and time-consuming tools. Moreover, in these cases it is necessary to know what to find in order to set up the experiment and to organize all the specific primers or antibodies to use against peculiar genes or proteins respectively. Therefore, in the current contest, Fourier Transform Infrared Microspectroscopy (FTIRM) represents an advantage from this point of view, offering at the same time qualitative and semi-quantitative analysis of an unknown sample, allowing to collect all the information about its composition. In fact, FTIRM being a high-resolution tool can provide relevant and reliable information at a molecular level on the whole macromolecular signature of cells and tissues, useful for the identification of spectral biomarkers specific for the different lesions [28,30–33]. Furthermore, with a single acquisition, which takes only few minutes, it is possible to obtain reliable information at a molecular level on the lipid and protein components, as well as on carbohydrates and nucleic acids. This analysis does not allow an absolute quantification, but it is very useful to detect even subtle changes in the relative amount and structure of the different macromolecules by comparing pathological samples with control ones. The possibility of obtaining so much information in a short time and with a single analysis is extremely useful for focusing the research on the most interesting topics.

In the present study, we propose a multifaceted approach combining Fourier Transform InfraRed Microspectroscopy (FTIRM) with multivariate and univariate analyses able to (1) identify specific spectral markers useful for discriminating between leiomyoma and leiomyosarcoma cell lines, also in comparison with healthy myometrium cells, and (2) deepen the effects of EPA and DHA supplements on these cell lines.

2. Materials and methods

Myometrium and leiomyoma cell lines (respectively A00-9 and A00-10) were kindly provided by William H. Catherino, M.D., Ph.D. (Department of Obstetrics and Gynecology, Uniformed Services University of the Health Sciences, Bethesda, Maryland). They were immortalized following a well assessed protocol [34] and modified using human papillomavirus type 16 [35]. Leiomyosarcoma cell lines (SKLMS-1) were purchased from ATCC (Manassas, Virginia, USA). *Cis*-5,8,11,14,17-eicosapentaenoic acid (EPA) and cis-4,7,10,13,16,19-docosahexaenoic acid (DHA) were purchased from Sigma–Aldrich (St. Louis, MO).

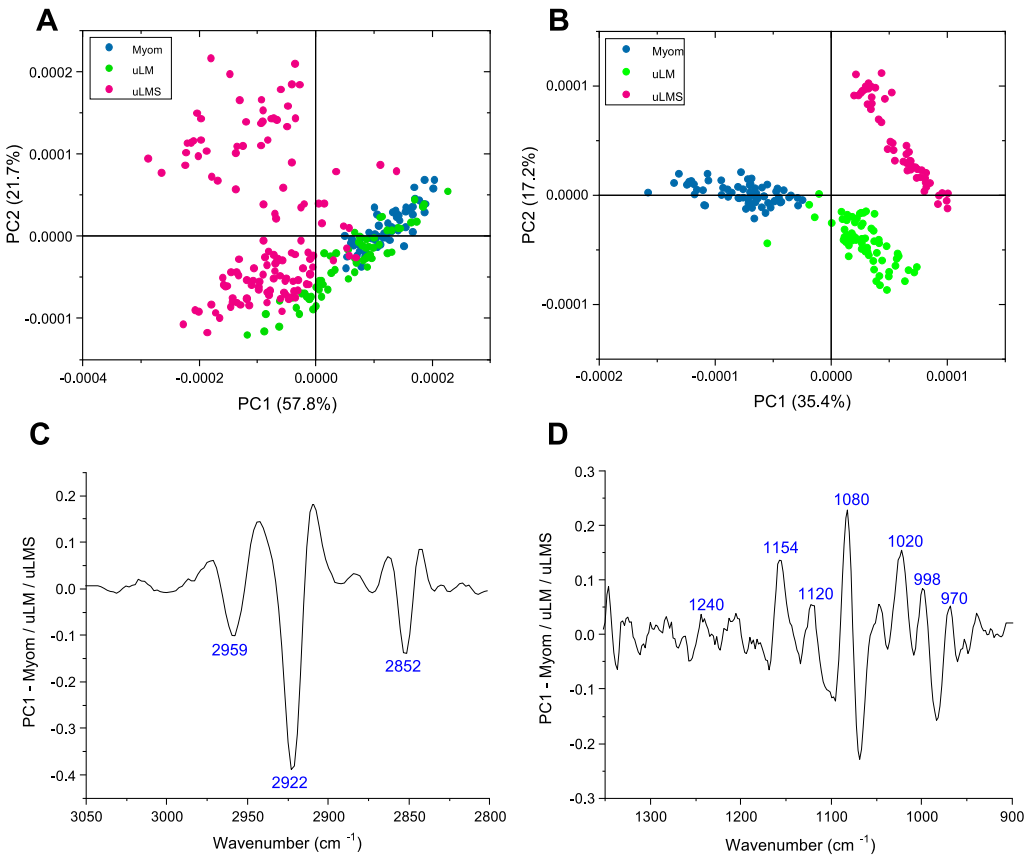

Fig. 2. PCA scores plots and corresponding PC1 loadings calculated on myometrium (Myom; blue dots), leiomyoma (uLM; green dots), and leiomyosarcoma (uLMS; magenta dots) spectral populations in the 3050–2800 cm^{-1} (A, C), and 1310–900 cm^{-1} (B, D) spectral regions.

2.1. Cell lines culture and treatments

Myometrium (Myom), leiomyoma (uLM) and leiomyosarcoma (uLMS) cells were cultured at 37 °C in a humidified atmosphere with 5 % CO_2 in fresh Dulbecco Modified Eagle Medium (DMEM-F12 Corning, New York, USA) supplemented with 10 % Fetal Bovine Serum (FBS, Euroclone, Milan, Italy), 1 % antibiotic (penicillin–streptomycin; Euro-Clone). Only myometrium and leiomyoma cells were also treated with 1 % fungizone (amphotericin B; Euroclone), and 1 % glutamine (Gibco, Life Technologies).

Myom, uLM, and uLMS cells were seeded in 96-well plates at initial densities of 1000 cells per well in total volume of 0.5 ml DMEM/F12 supplemented with 10 % FBS for myometrium and leiomyoma cells, and DMEM low glucose supplemented with 10 % FBS for leiomyosarcoma ones. Two aliquots of each cell line were treated respectively with EPA 50 μM (named Myom-EPA, uLM-EPA, and uLMS-EPA), and DHA 50 μM (named Myom-DHA, uLM-DHA, and uLMS-DHA) and incubated at 37 °C in a humidified atmosphere with 5 % of CO_2 for 48 h [28], while the third one, taken as control, was normally cultured without treatments (named Myom, uLM, and uLMS).

2.2. Cell viability assay: MTT test

MTT (3-(4,5-dimethylthiazol–2-yl)-2,5-diphenyltetrazolium bromide) assay was used to evaluate cell proliferation in all experimental groups. This assay is based on the reduction of the tetrazolium salt by intracellular dehydrogenases of viable living cells, leading to the formation of purple formazan crystals. Control (Myom, uLM, and uLMS groups) and EPA (Myom-EPA, uLM-EPA, and uLMS-EPA groups) and DHA (Myom-DHA, uLM-DHA, and uLMS-DHA groups) treated cells were washed with PBS and incubated with MTT solution at 0.5 mg/ml for 3 h at 37 °C. The medium was then removed, and the crystals were dissolved in isopropyl alcohol acidified with HCl. In the final step, absorbance was measured at 570 nm using Multiskan GO microplate reader (Thermo Scientific).

2.3. Fourier Transform InfraRed Microspectroscopy measurements

FTIRM measurements were performed using an Invenio-R interferometer coupled with a Hyperion 3000 Vis-IR microscope, equipped with a HgCdTe (MCT) detector operating at liquid nitrogen temperature (Bruker Optics, Ettlingen, Germany).

For FTIRM analysis, each cell line was treated with EPA and DHA as described in Section 2.1, was then harvested, formalin fixed (PFA 4 %) and stored at 4 °C in physiological solution (NaCl 0.9 %). The experiment was carried out in triplicate. Before starting measurements, cells were washed twice with MilliQ water and centrifuged at 800*g* for 10 min each. Then, an aliquot of ~10 μl of pellet was collected from each experimental group, spotted onto CaF_2 optical windows (1 mm thick, 13 mm diameter) and let air dry for 20 min before the acquisition.

For each sample, ~60 densely packed microareas of 30 × 30 mm^2 were selected by using the television camera. IR spectra were acquired in transmission mode in the 4000–700 cm^{-1} spectral interval (512 scans, spectral resolution 4 cm^{-1}). Before each acquisition, a background spectrum was collected with the same parameters on a clean portion of the CaF_2 optical window. Raw spectra were first submitted to water vapor and atmospheric compensation routine, vector normalized and interpolated in the 3050–2800 cm^{-1}, 1760–1350 cm^{-1}, and 1310–900 cm^{-1} ROI (Regions Of Interest), respectively related to lipid, proteins, and carbohydrates/nucleic acids (OPUS 7.5 software, Bruker Optics, Ettlingen, Germany).

Table 2
Statistical analysis of band area ratios calculated for myometrium (Myom), leiomyoma (uLM) and leiomyosarcoma (uLMS) cellular groups. Values are reported as mean values ± S.D. (statistical significance was set at $p < 0.05$).

	Myom	uLM	uLMS	*p* values
A_{3014}/A_{2959}	0.0107 ± 0.0012	0.0301 ± 0.0031	0.0184 ± 0.0023	Myom *vs* uLM p < 0.0001 Myom *vs* uLMS *p* < 0.001 uLM *vs* uLMS p < 0.0001
A_{2923}/A_{2959}	2.323 ± 0.233	2.211 ± 0.223	1.589 ± 0.159	Myom *vs* uLM p > 0.05 Myom *vs* uLMS p < 0.001 uLM *vs* uLMS *p* < 0.01
A_{1740}/A_{TOT}	0.000276 ± 0.000031	0.000286 ± 0.000034	0.000164 ± 0.000020	Myom *vs* uLM p > 0.05 Myom *vs* uLMS p < 0.001 uLM *vs* uLMS p < 0.0001
A_{1172}/A_{1156}	0.405 ± 0.044	1.109 ± 0.112	0.862 ± 0.088	Myom *vs* uLM p < 0.0001 Myom *vs* uLMS p < 0.001 uLM *vs* uLMS p < 0.01
A_{1058}/A_{TOT}	0.207 ± 0.021	0.216 ± 0.022	0.219 ± 0.023	Myom *vs* uLM p > 0.05 Myom *vs* uLMS *p* > 0.05 uLM *vs* uLMS p > 0.05
A_{965}/A_{1080}	0.0306 ± 0.0031	0.0383 ± 0.0039	0.0459 ± 0.0046	Myom *vs* uLM p < 0.05 Myom *vs* uLMS p < 0.001 uLM *vs* uLMS p < 0.05
A_{927}/A_{965}	0.1634 ± 0.0175	0.1339 ± 0.0156	0.0435 ± 0.0016	Myom *vs* uLM p < 0.05 Myom *vs* uLMS p < 0.0001 uLM *vs* uLMS p < 0.0001
A_{992}/A_{1080}	0.1568 ± 0.0159	0.1469 ± 0.0148	0.1648 ± 0.0169	Myom *vs* uLM p > 0.05 Myom *vs* uLMS p > 0.05 uLM *vs* uLMS *p* > 0.05

2.4. IR data analysis

Preprocessed spectra were converted in Second Derivative mode (Savitzky–Golay filter, 9 points of smoothing), and submitted to Principal Component Analysis to analyze in an unsupervised manner the different spectral populations. PCA scores plots and PC1 loadings were calculated in the above-defined ROI (OriginPro 2023 software, OriginLab Corporation, Northampton, MA, USA).

Moreover, for each experimental group, the mean average spectrum and the relative average spectra ± standard deviation spectra were calculated and submitted to peak fitting procedure, which is fundamental to perform a correct vibrational analysis of biological samples. In fact, IR bands are often convoluted because they derive from the overlapping of several peaks, generated from different vibrational modes, but with similar wavenumbers. The number and position (expressed as wavenumbers) of all the peaks lie under the 3050–2800 cm^{-1}, 1760–1350 cm^{-1}, and 1310–900 cm^{-1} ROI were identified by second derivative minima analysis and fixed during the fitting procedure (GRAMS/AI 9.1, Galactic Industries, Inc., Salem, New Hampshire). A Gaussian function was adopted; the integrated areas of all the underlying peaks were obtained and used to calculate specific band area ratios (see Results section).

2.5. Statistical analysis

Normally distributed data were reported as mean ± S.D. The factorial analysis of variance (One-way ANOVA) was applied and significant differences among groups determined (GraphPad Software, Inc., San Diego, CA, USA). Statistical significance was set at $p < 0.05$, and different letter over the box indicate statistically significant values among cells of the same cell line differently treated.

3. Results

3.1. FTIRM characterization of myometrium (Myom), leiomyoma (uLM) and leiomyosarcoma (uLMS) cell lines

In Fig. 1, the second derivative average spectra of Myom, uLM and uLMS cell lines are reported; spectra are displayed in second derivative mode in the 3050–2800 cm^{-1}, 1780–1480 cm^{-1}, and 1310–900 cm^{-1} spectral regions, related respectively to lipids, proteins, and nucleic acids/carbohydrates. The main peaks are labeled and assigned as reported in Table 1.

Then, the spectral populations of the three cell lines (Myom, uLM and uLMS) were submitted to Principal Component Analysis to identify the main sources of variation. The analysis was performed in three different spectral regions; the PCA scores plots and the corresponding PC1 loadings are reported in Fig. 2. As regards the 3050–2800 cm^{-1} interval, representative of the vibrational modes of lipid alkyl chains, the PCA scores plot indicates only a weak segregation between uLMS cells and Myom and uLM ones along the PC1 axis (explained variance 57.8 %); Myom and uLM cells resulted partially overlapped (Fig. 2A). No segregation was found among the three cell lines in the 1760–1350 cm^{-1} spectral range, diagnostic of the protein pattern (data not shown). Finally, a clear discrimination was observed in the 1310–900 cm^{-1} spectral range, representative of nucleic acids and carbohydrates (Fig. 2B): PC1 divided Myom cells from tumoral ones (uLM and uLMS), with an explained variance of 35.4 %, while PC2 segregated uLM form uLMS (explained variance 17.2 %). These results were also confirmed by the analysis of the PC1 loadings, which evidenced some spectral differences among groups, mainly in the lipid component (Fig. 2C) and in nucleic acids and carbohydrates (Fig. 2D).

Based on the analysis of PC1 loadings, the following band/area ratios were calculated and statistically analyzed to identify reliable spectral biomarkers able to discriminate among the healthy cells of myometrium, and the benign and malignant ones of leiomyoma and leiomyosarcoma: A_{3014}/A_{2959} (ratio between the areas of the bands at 3014 cm^{-1} and 2959 cm^{-1}; unsaturated lipid fraction) [31]; A_{2923}/A_{2959} (ratio between the areas of the bands at 2923 cm^{-1} and 2959 cm^{-1}; saturated lipid fraction) [31,32]; A_{1740}/A_{TOT} (ratio between the area of the band at 1740 cm^{-1} and TOT, which means the sum of the integrated area of the whole 1800–900 cm^{-1} range; fatty acids) [32]; A_{1172}/A_{1156} (ratio between the areas of the bands at 1172 cm^{-1} and 1156 cm^{-1}; phosphorylated compounds) [30,31]; A_{1058}/A_{TOT} (ratio between the areas of the bands at 1058 cm^{-1} and TOT, already defined; carbohydrates) [31,32]; A_{992}/A_{1080} (ratio between the areas of the bands at 992 cm^{-1} and 1080 cm^{-1}; RNA) [30]; A_{965}/A_{1080} (ratio between the areas of the bands at 965 cm^{-1} and 1080 cm^{-1}; A-DNA) [44] and A_{927}/A_{965} (ratio between the areas of the bands at 927 cm^{-1} and 965 cm^{-1}; *Z*-DNA) [31]. The mean values ± S.D calculated for myometrium, leiomyoma, and leiomyosarcoma cells are reported in Table 2.

For a better comprehension, the numerical variation of the above defined spectral parameters is also shown in Fig. 3. Leiomyoma cells were mostly characterized by high amounts of lipids: in particular, they displayed the highest and statistically significant level of unsaturated

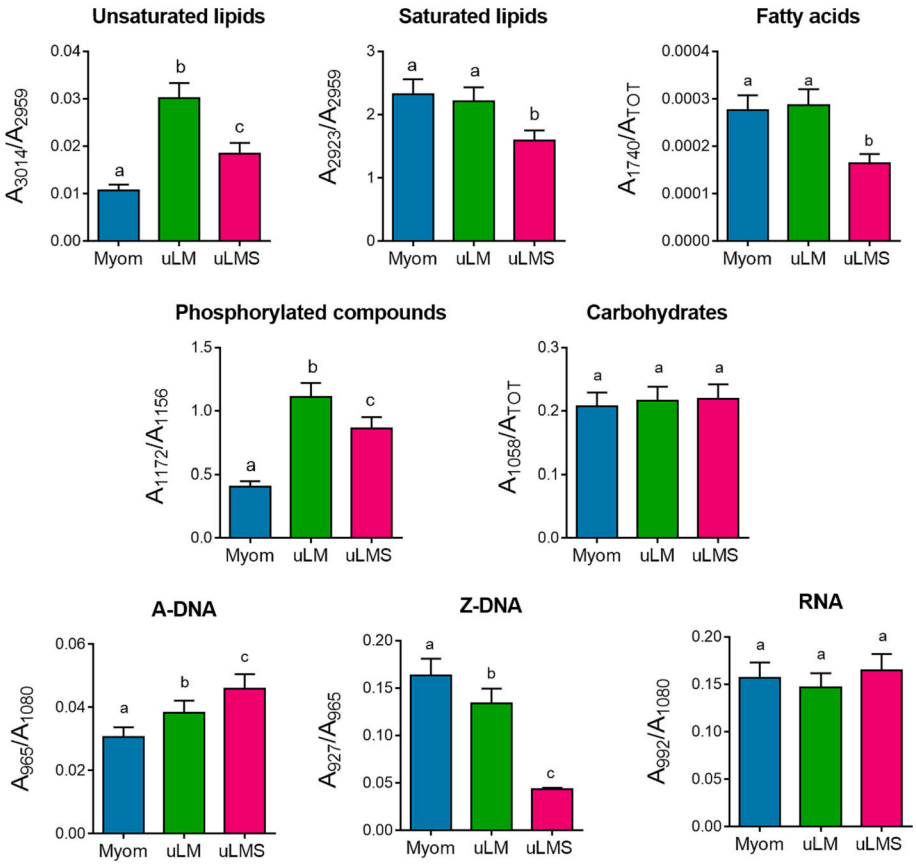

Fig. 3. Band/area ratios calculated on myometrium (Myom; blue), leiomyoma (uLM; green) and leiomyosarcoma (uLMS; magenta) spectral populations: A_{3014}/A_{2959} (Unsaturated lipids); A_{2923}/A_{2959} (Saturated lipids); A_{1740}/A_{TOT} (Fatty acids); A_{1172}/A_{1156} (Phosphorylated compounds); A_{1058}/A_{TOT} (Carbohydrates); A_{965}/A_{1080} (A-DNA); A_{927}/A_{965} (Z-DNA), and A_{992}/A_{1080} (RNA). One-Way ANOVA was performed among groups. Different letters over histograms mean statistically significant values (statistical significance was set at $p < 0.05$).

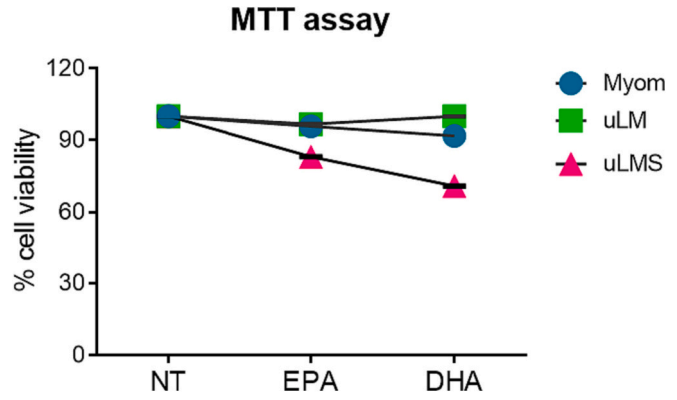

Fig. 4. Cell viability percentage curves of Myom (blue circles lines), uLM (green squares lines), and uLMS (magenta triangles lines) cell lines treated as follows: no treatment (NT); 48 h in EPA 50 μM (EPA), and 48 h in DHA 50 μM (DHA).

alkyl chains (A_{3014}/A_{2959} ratio), while the levels of saturation (A_{2923}/A_{2959} ratio) and fatty acids (A_{1740}/A_{TOT} ratio) were similar to those showed by myometrium cell lines, but higher respect to leiomyosarcoma ones. Leiomyoma cells displayed also the highest level of phosphorylated compounds (A_{1172}/A_{1156} ratio). Leiomyosarcoma cells recorded the highest DNA content (A_{965}/A_{1080} ratio), but at the same time the lowest in terms of *Z*-DNA, *i.e.* the methylated DNA conformation, (A_{927}/A_{965} ratio), thus confirming the increased level of RNA (A_{992}/A_{1080} ratio) respect to myometrium and leiomyoma, even if not statistically significant. No significant changes able to discriminate among groups were found also in the carbohydrate's ratio (A_{1058}/A_{TOT} ratio).

3.2. Evaluation of EPA and DHA treatments on myometrium (Myom), leiomyoma (uLM) and leiomyosarcoma (uLMS) cell lines

The effects induced in Myom, uLM, and uLMS cell lines by 48 h of treatment with EPA and DHA, were first analyzed through the MTT assay, which let estimate the vitality of cells. As reported in Fig. 4, the percentage of cell viability clearly decreased in leiomyosarcoma cells treated with EPA and, even more, with DHA, while it remained almost the same for myometrium and leiomyoma ones.

To appreciate the effects induced by EPA and DHA at lipid and nucleic acids level, and to investigate if they could act with a different mechanism in healthy, benign, and malignant cells, the IR spectra of the three cell lines treated with EPA and DHA were submitted to PCA in the 3050–2800 cm^{-1} and 1310–900 cm^{-1} spectral regions (Fig. 5). More in detail, as regard the 3050–2800 cm^{-1} range (related to lipids), for all the cell lines, the main segregation was found only between DHA treated (Myom-DHA, uLM-DHA, and uLMS-DHA) and not treated (Myom, uLM, and uLMS) cells, with EPA treated ones (Myom-EPA, uLM-EPA, and uLMS-EPA) in an intermediate position and partially overlapped to not treated ones (Fig. 5A, E, I). As regards the 1310–900 cm^{-1} spectral region, treatments seemed to not affect the nucleic acids and carbohydrates composition of healthy cells, with EPA and DHA treated myometrium cells (Myom-EPA and Myom-DHA) displaying only a weak segregation from not treated ones (Myom) (Fig. 5B). Conversely, a good separation was observed in leiomyoma and leiomyosarcoma cell lines in relation with the treatment: both EPA (uLM-EPA and uLMS-EPA) and DHA (uLM-DHA and uLM-DHA) treated cells were clearly segregated respect to not treated ones (Fig. 5F, L). As regards PC1 loadings, the loading plots in the lipid range highlighted that the segregation was mainly due to variations related to unsaturated and saturated lipid fractions, *i.e.* changes in aliphatic chain lengths (Fig. 5C, G, M). About the second ROI considered, the situation is not so homogenous: in

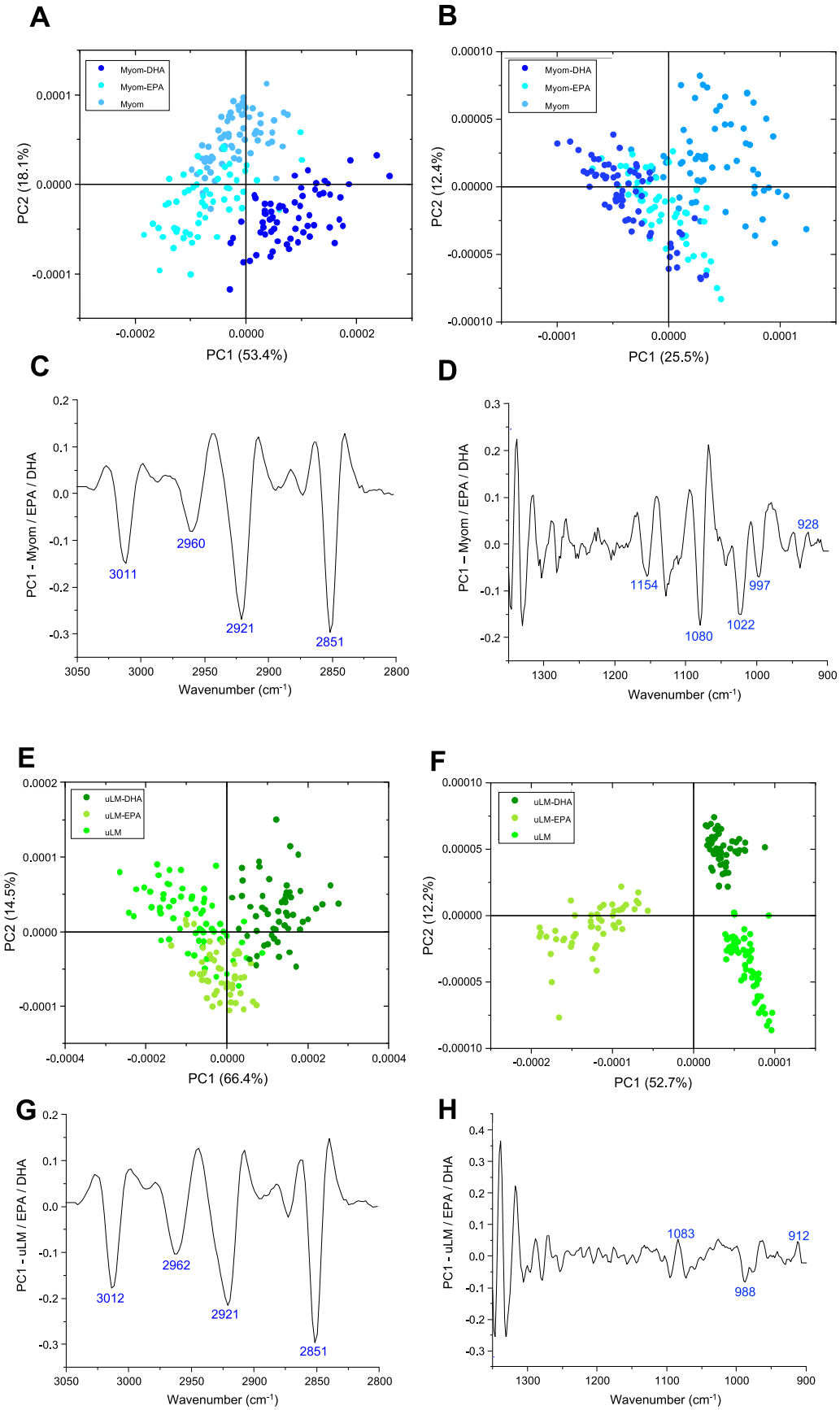

Fig. 5. PCA scores plots and corresponding PC1 loadings calculated on the following spectral populations: Myom, Myom-EPA and Myom-DHA in the 3050–2800 cm^{-1} (A, C) and 1310–900 cm^{-1} (B, D) spectral ranges; uLM, uLM-EPA and uLM-DHA in the 3050–2800 cm^{-1} (E, G) and 1310–900 cm^{-1} (F, H) spectral ranges, and uLMS, uLMS-EPA and uLMS-DHA in the 3050–2800 cm^{-1} (I; M) and 1310–900 cm^{-1} (L, N) spectral ranges.

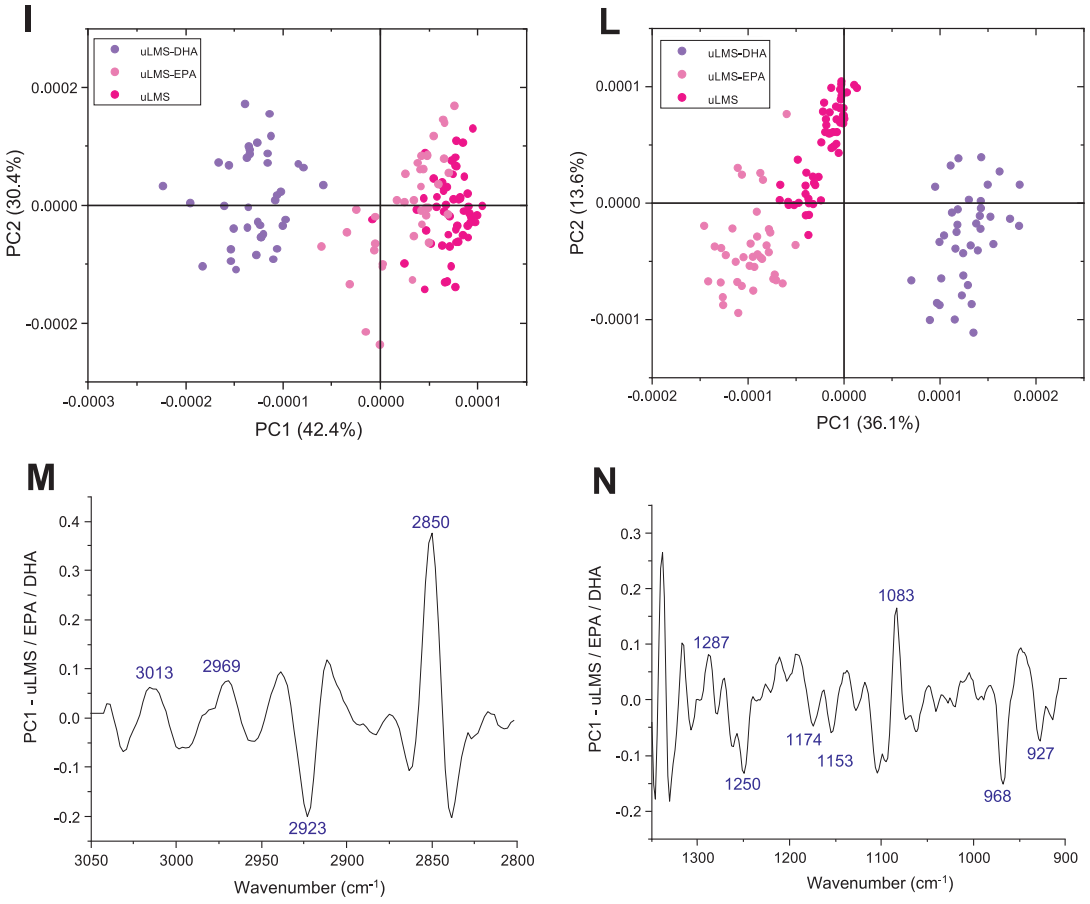

Fig. 5. (*continued*).

healthy myometrial cells, the segregation along the PC1 seems to be ascribable for the most to carbohydrate moieties, followed by contributions related to DNA and phosphates (Fig. 5D). These contributions are more evident in leiomyosarcoma, together with that related to phosphorylated compounds (Fig. 5H, N).

To assess the effects induced by EPA and DHA omega-3 fatty acids on the tested cell lines, the univariate statistical analysis was focused on the above defined band area ratios, related to the degree of saturation and unsaturation of lipid alkyl chains, the relative amount of carbohydrates and phosphorylated compounds, as well as to DNA and RNA changes in conformation and composition. The mean values ± S.D. calculated for myometrium, leiomyoma, and leiomyosarcoma cells before (NT) and after EPA and DHA treeatments are reported in Tables 3-5 (respectively for myometrium, leiomyoma, and leiomyosarcoma cells).

For a better comprehension, the numerical variation of the above defined spectral parameters is also shown in Fig. 6. About the lipid component, all the tested cell lines displayed an increase in the unsaturation levels (A_{3014}/A_{2959} ratio) after both EPA and DHA treatments: this increment was more pronounced in uLM-DHA and uLMS-DHA, than in Myom-DHA; a similar but even less evident trend was observed in the saturated lipid fraction (A_{2923}/A_{2959} ratio). Both these results, together with the increase of the relative amount of fatty acids (A_{1740}/A_{TOT} ratio) in all treated samples, suggested the uptake of EPA and DHA by the tested cell lines. The A_{1172}/A_{1156} ratio is referred to the phosphorylation level of C—O groups, considered as an oxidative marker typical of the neoplastic behavior; interestingly, all EPA-treated samples (uLM-EPA, uLMS-EPA, and Myom-EPA) registered higher values of this parameter, respect to DHA (uLM-DHA, uLMS-DHA, and Myom-DHA) and not treated (uLM, uLMS, and Myom) ones. Higher levels of carbohydrates (A_{1058}/A_{TOT} ratio) were found in leiomyoma (uLM-DHA) and, to a major extent, leiomyosarcoma (uLMS-DHA) cells respect to healthy ones (Myom-DHA), after treatment with DHA. As regards nucleic acids, only a decrease in *Z*-DNA was observed in uLMS-DHA, while no statistically significant variation in the relative amount of A-DNA (A_{965}/A_{1080}) was observed in all the treated samples. Finally, an inverse trend in the relative amount of RNA (A_{992}/A_{1080} ratio) was observed in leiomyoma and leiomyosarcoma cell lines after omega 3-fatty acids treatments: uLM-EPA and uLM-DHA displayed the lowest values, while uLMS-EPA asnd uLMS-DHA, the highest ones; no statistically significant changes were observed in Myom-EPA and Myom-DHA, respect to not treated cells.

4. Discussion

Gynecological diseases represent an important burden affecting women in fertile and perimenopausal age, with social and economic impacts due to fertility problems and to the number of hospitalizations with surgical interventions linked to them [48,49]. In less severe cases, hormonal and in general pharmacological therapies remain the treatment of choice to avoid worsening and to ease the pain and symptomatology from them [5,50].

Still today, despite the improvement in imaging diagnostic techniques, the crucial issue related to uterine neoplasms relies on the difficulty to distinguish them through the current clinical diagnostic tests before surgery [7,9]. In fact, uterine leiomyoma and leiomyosarcoma arise from the myometrial smooth muscle cells; they share symptomatology and appearance but a very different prognosis, hence the conservative management of the benign lesion can often lead to the misdiagnosis of a possible malignancy resulting in significant delays in the beginning of appropriate treatments, and increasing patient

Table 3
Statistical analysis of band area ratios calculated for myometrium (Myom) cells before (NT) and after EPA and DHA treatments. Values are reported as mean values ± S.D. (statistical significance was set at $p < 0.05$).

	Myom			p values
	NT	EPA	DHA	
A_{3014}/A_{2959}	0.0107 ± 0.0012	0.0179 ± 0.0021	0.0294 ± 0.0032	Myom-NT *vs* Myom-EPA $p < 0.001$ Myom-NT *vs* Myom-DHA p < 0.0001 Myom-EPA *vs* Myom-DHA p < 0.0001
A_{2923}/A_{2959}	2.323 ± 0.233	2.222 ± 0.225	2.413 ± 0.248	Myom-NT *vs* Myom-EPA p > 0.05 Myom-NT *vs* Myom-DHA $p > 0.05$ Myom-EPA *vs* Myom-DHA $p > 0.05$
A_{1740}/A_{TOT}	0.000276 ± 0.000031	0.000403 ± 0.000050	0.000677 ± 0.000072	Myom-NT *vs* Myom-EPA $p < 0.01$ Myom-NT *vs* Myom-DHA p < 0.0001 Myom-EPA *vs* Myom-DHA $p < 0.0001$
A_{1172}/A_{1156}	0.405 ± 0.044	0.668 ± 0.069	0.546 ± 0.057	Myom-NT *vs* Myom-EPA p < 0.0001 Myom-NT *vs* Myom-DHA p < 0.01 Myom-EPA *vs* Myom-DHA p < 0.05
A_{1058}/A_{TOT}	0.207 ± 0.021	0.230 ± 0.025	0.251 ± 0.027	Myom-NT *vs* Myom-EPA p > 0.05 Myom-NT *vs* Myom-DHA p < 0.05 Myom-EPA *vs* Myom-DHA p > 0.05
A_{965}/A_{1080}	0.0306 ± 0.0031	0.0344 ± 0.0034	0.0337 ± 0.0034	Myom-NT *vs* Myom-EPA p > 0.05 Myom-NT *vs* Myom-DHA p > 0.05 Myom-EPA *vs* Myom-DHA p > 0.05
A_{927}/A_{965}	0.1634 ± 0.0175	0.1377 ± 0.0148	0.1769 ± 0.0019	Myom-NT *vs* Myom-EPA p > 0.05 Myom-NT *vs* Myom-DHA p > 0.05 Myom-EPA *vs* Myom-DHA p < 0.01
A_{992}/A_{1080}	0.1568 ± 0.0176	0.1709 ± 0.0148	0.1605 ± 0.0162	Myom-NT *vs* Myom-EPA p > 0.05 Myom-NT *vs* Myom-DHA p > 0.05 Myom-EPA *vs* Myom-DHA p > 0.05

Table 4
Statistical analysis of band area ratios calculated for leiomyoma (uLM) cells before (NT) and after EPA and DHA treatments. Values are reported as mean values ± S.D. (statistical significance was set at $p < 0.05$).

	uLM			p values
	NT	EPA	DHA	
A_{3014}/A_{2959}	0.0301 ± 0.0031	0.0328 ± 0.0032	0.0389 ± 0.0041	uLM-NT *vs* uLM-EPA $p > 0.05$ uLM-NT *vs* uLM-DHA p < 0.001 uLM-EPA *vs* uLM-DHA p < 0.01
A_{2923}/A_{2959}	2.211 ± 0.223	2.286 ± 0.229	2.4461 ± 0.248	uLM-NT *vs* uLM-EPA $p > 0.05$ uLM-NT *vs* uLM-DHA $p > 0.05$ uLM-EPA *vs* uLM-DHA p > 0.05
A_{1740}/A_{TOT}	0.000286 ± 0.000034	0.000409 ± 0.000045	0.000712 ± 0.000075	uLM-NT *vs* uLM-EPA p < 0.05 uLM-NT *vs* uLM-DHA p < 0.0001 uLM-EPA *vs* uLM-DHA p < 0.0001
A_{1172}/A_{1156}	1.109 ± 0.112	1.121 ± 0.114	0.947 ± 0.107	uLM-NT *vs* uLM-EPA p > 0.05 uLM-NT *vs* uLM-DHA $p > 0.05$ uLM-EPA *vs* uLM-DHA p > 0.05
A_{1058}/A_{TOT}	0.216 ± 0.022	0.246 ± 0.026	0.295 ± 0.032	uLM-NT *vs* uLM-EPA p > 0.05 uLM-NT *vs* uLM-DHA p < 0.01 uLM-EPA *vs* uLM-DHA p < 0.05
A_{965}/A_{1080}	0.0383 ± 0.0039	0.0403 ± 0.0040	0.0416 ± 0.0042	uLM-NT *vs* uLM-EPA p > 0.05 uLM-NT *vs* uLM-DHA $p > 0.05$ uLM-EPA *vs* uLM-DHA p > 0.05
A_{927}/A_{965}	0.1339 ± 0.0156	0.1443 ± 0.0159	0.1372 ± 0.0152	uLM-NT *vs* uLM-EPA p > 0.05 uLM-NT *vs* uLM-DHA $p > 0.05$ uLM-EPA *vs* uLM-DHA p > 0.05
A_{992}/A_{1080}	0.1469 ± 0.0148	0.1287 ± 0.0129	0.1285 ± 0.0129	uLM-NT *vs* uLM-EPA $p > 0.05$ uLM-NT *vs* uLM-DHA p > 0.05 uLM-EPA *vs* uLM-DHA p > 0.05

morbidity and mortality [2]. For this reason, in terms of treatments, the golden standard still remains the surgical removal even not always as the definite therapy, given the risk of recurrence.

Polyunsaturated omega-3 fatty acids are well assessed supplements used in the prevention of several cardiovascular, neurological, and inflammatory disorders and, only recently, also to fight cancer. Among them, eicosapentaenoic and docosahexaenoic acids, better known respectively as EPA and DHA, have recently been reported for having positive effects in the treatment of uterine leiomyoma or in several other types of cancers [16,21,23,51–53].

Based on these findings, the present work aimed to probe the

Table 5
Statistical analysis of band area ratios calculated for leiomyosarcoma (uLMS) cells before (NT) and after EPA and DHA treatments. Values are reported as mean values ± S.D. (statistical significance was set at $p < 0.05$).

	uLMS			p values
	NT	EPA	DHA	
A_{3014}/A_{2959}	0.0184 ± 0.0023	0.0207 ± 0.0022	0.0318 ± 0.0034	uLMS-NT *vs* uLMS-EPA p > 0.05 uLMS-NT *vs* uLMS-DHA p < 0.0001 uLMS-EPA *vs* uLMS-DHA p < 0.0001
A_{2923}/A_{2959}	1.589 ± 0.159	1.806 ± 0.183	2.009 ± 0.203	uLMS-NT *vs* uLMS-EPA p > 0.05 uLMS-NT *vs* uLMS-DHA p < 0.01 uLMS-EPA *vs* uLMS-DHA p > 0.05
A_{1740}/A_{TOT}	0.000164 ± 0.000020	0.000274 ± 0.000033	0.000945 ± 0.000113	uLMS-NT *vs* uLMS-EPA p > 0.05 uLMS-NT *vs* uLMS-DHA *p* < 0.0001 uLMS-EPA *vs* uLMS-DHA *p* < 0.0001
A_{1172}/A_{1156}	0.862 ± 0.088	1.051 ± 0.120	0.749 ± 0.059	uLMS-NT *vs* uLMS-EPA p < 0.05 uLMS-NT *vs* uLMS-DHA p > 0.05 uLMS-EPA *vs* uLMS-DHA p < 0.001
A_{1058}/A_{TOT}	0.219 ± 0.023	0.256 ± 0.026	0.342 ± 0.035	uLMS-NT *vs* uLMS-EPA p > 0.05 uLMS-NT *vs* uLMS-DHA p < 0.0001 uLMS-EPA *vs* uLMS-DHA p < 0.01
A_{965}/A_{1080}	0.0459 ± 0.0046	0.0461 ± 0.0047	0.0485 ± 0.0048	uLMS-NT *vs* uLMS-EPA p > 0.05 uLMS-NT *vs* uLMS-DHA *p* > 0.05 uLMS-EPA *vs* uLMS-DHA p > 0.05
A_{927}/A_{965}	0.0435 ± 0.0016	0.0652 ± 0.0686	0.0099 ± 0.0012	uLMS-NT *vs* uLMS-EPA p < 0.0001 uLMS-NT *vs* uLMS-DHA *p* < 0.0001 uLMS-EPA *vs* uLMS-DHA p < 0.0001
A_{992}/A_{1080}	0.1648 ± 0.0169	0.2034 ± 0.0215	0.2091 ± 0.0218	uLMS-NT *vs* uLMS-EPA p < 0.05 uLMS-NT *vs* uLMS-DHA p < 0.05 uLMS-EPA *vs* uLMS-DHA p > 0.05

potential of the Fourier Transform InfraRed Microscopy in the investigation of uterine leiomyoma and leiomyosarcoma cells, with the dual purpose of detecting reliable tumor-specific spectral biomarkers able to distinguish among the benign leiomyoma, and the malignant leiomyosarcoma, and exploring the effects of EPA and DHA administration on the same cells in terms of macromolecular composition.

Results revealed that it is possible to distinguish among the three different cell populations, by the identification of several spectral biomarkers related to the unsaturated and saturated lipid fractions, the presence of phosphorylated compounds, and nucleic acids conformation. Meanwhile, the uptake of EPA and DHA seems to be confirmed by the increase of the A_{1740}/A_{TOT} ratio in all three cell lines especially in leiomyosarcoma after DHA treatment and with a superimposed trend between leiomyoma and myometrium. In a similar way, the performance of carbohydrates with an equivalent situation in not treated and EPA treated cells, highlighting a stronger effect of DHA above all in malignant cells. The highest ratio of leiomyosarcoma in terms of A-DNA showed an increased replication in these malignant cells respect to leiomyoma cells and to a greater extent respect to the myometrial ones, without being affected by omega-3 administration. Leiomyosarcoma cells showed more DNA content respect to the healthy and benign lines but less methylated, as confirmed by the *Z*-DNA ratio, which showed inverted trends respect to A-DNA. EPA treatment decreases the methylation level of myometrium and leiomyoma cells but increases those of malignant cells; an opposite trend was found after the DHA treatment. Even if no differences were found in all three cell lines before treatments, EPA and DHA seem to affect differently the RNA level in both uterine lesions. All these findings let hypothesize higher replication and transcription rates in malignant cells respect to the other two cell lines, even after omega-3 administration, but also that their DNA is less methylated respect to the one found in leiomyoma and myometrium cells, thus strengthening, and supporting the highest RNA content.

This suggests not only that each omega-3 exerts different effects on the same cell line, maybe just due to their different chemical structure, but also that EPA and DHA, considered alone, can induce reverse effects among myometrium, leiomyoma, and leiomyosarcoma. This could be ascribed to the different nature of the three cell lines considered, that even belong to the same uterine district, it is evident that they variously respond to the omega-3 treatments. It is evident that the most striking event is the one observed at the lipid level and therefore up to the cell membrane, together with the result that myometrium cells appear to undergo minor changes induced by the treatments, as displayed by the lack of evidenced significant spectral changes. Conversely, contrary to what is already reported in the literature about other forms of cancer, DHA seems to enhance leiomyosarcoma cells with positive effects [23]. In this malignant cell line in fact, both supplements lead to the increase of carbohydrates (A_{1058}/A_{TOT} ratio), simultaneously with a decrease of phosphorylated compounds after DHA (A_{1172}/A_{1156} ratio), with a slow increase of DNA (A_{965}/A_{1080} ratio) and with a growing transcription rate (A_{992}/A_{1080} ratio): this seems to display a clinical picture of cells not affected by the initially supposed antiproliferative or cytotoxic effects exerted by this omega-3 PUFA. On the other hand, EPA induced a similar influence on leiomyosarcoma but not so effective. Leiomyoma cells, instead, showed a condition quite always overlapped or more similar to that of healthy myometrium. In these benign tumor cells, EPA and DHA did not affect nucleic acids composition with statistically significant values, with DHA influenced for the most carbohydrates decreasing their phosphorylation rate, suggesting again its stronger impact respect to EPA.

All these results enrich the scenario previously depicted by the study involving both these omega-3 in leiomyoma tissue biopsies in which, since there, DHA demonstrated to be more effective in reducing the collagen impairment, and where myometrium tissue showed not to be affected by the impact of both fatty acids [28]. Leaving aside the apparent similarity of the two neoplasms, it is evident that there are mechanisms and characteristics that are very different from them, for

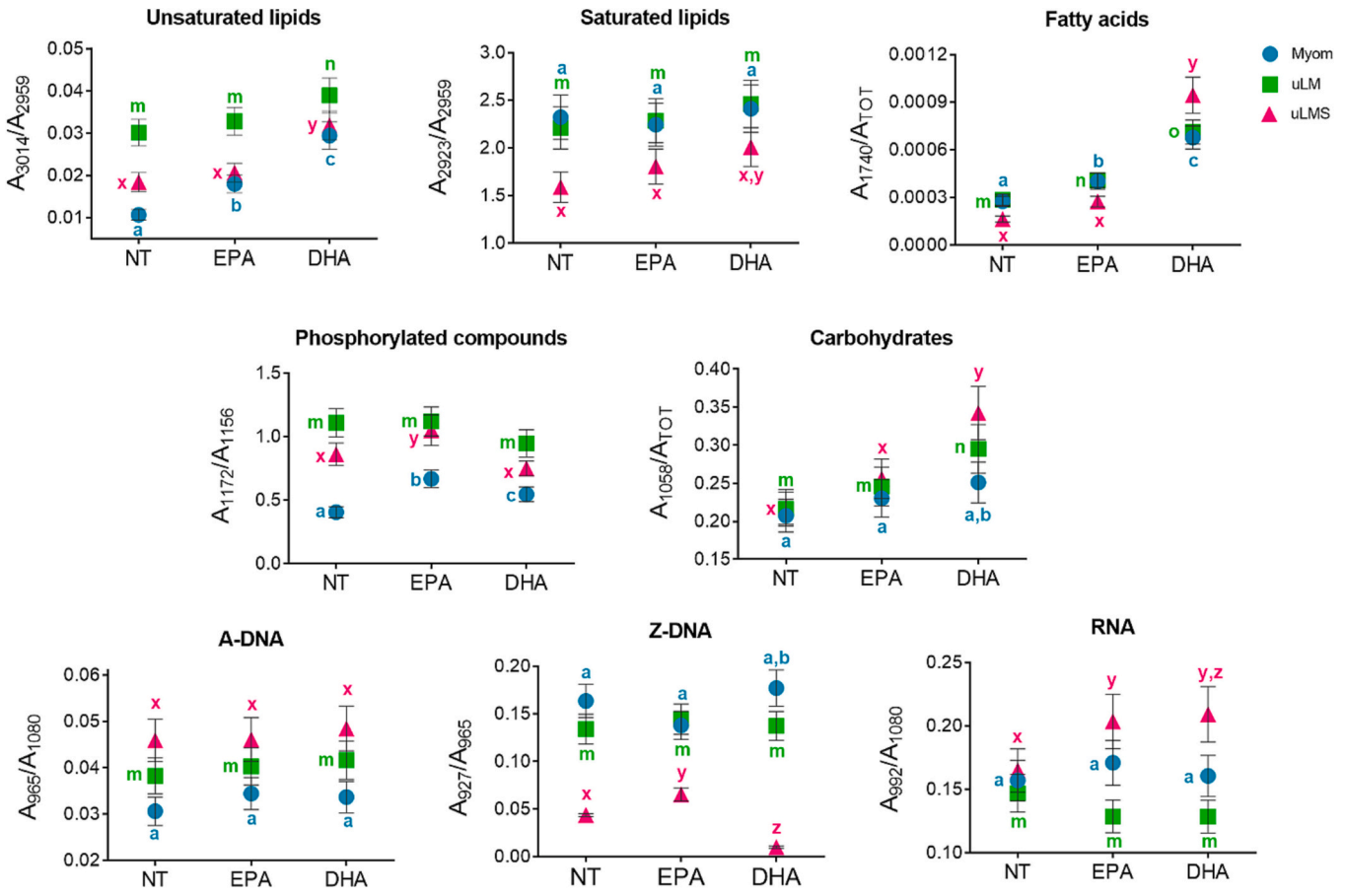

Fig. 6. Band area ratios calculated on myometrium (Myom; blue dots), leiomyoma (uLM; green squares) and leiomyosarcoma (uLMS; magenta triangles) spectral populations before (NT) and after EPA and DHA treatments: A_{3014}/A_{2959} (Unsaturated lipids); A_{2923}/A_{2959} (Saturated lipids); A_{1740}/A_{TOT} (Fatty acids); A_{1172}/A_{1156} (Phosphorylated compounds); A_{1058}/A_{TOT} (Carbohydrates); A_{965}/A_{1080} (A-DNA); A_{927}/A_{965} (*Z*-DNA), and A_{992}/A_{1080} (RNA). One-Way ANOVA was performed among groups. Different letters over histograms mean statistically significant values (statistical significance was set at $p < 0.05$).

which it will be necessary to deepen independently the cellular pathway involved by the administration of EPA and DHA. For sure, at the moment, EPA and DHA can better exert a beneficial role at a tissue level in reducing the overproduction of Extra Cellular Matrix, especially collagen. At present, for the first time to the authors' knowledge, this work represents the first FTIRM approach employed for the investigation of two uterine tumor lesions in an *in-vitro* experiment using cell lines, and at the same time the first step for the evaluation of a possible treatment strategy to be pursued in those undoubted cases. The next goals will cover the deepening of the effects of EPA and DHA through molecular approaches and the use of primary cells to avoid any inconvenience due to the repeated cultural passages. Moreover, as done for leiomyoma, leiomyosarcoma biopsy tissues will be investigated through a FTIR Imaging approach to find out more also at a tissue level.

5. Conclusions

The current study aimed to investigate two gynecological lesions, leiomyoma and leiomyosarcoma, finding novel and meaningful spectral biomarkers able to characterize both these lesions and to deepen the potential use of EPA and DHA omega-3 fatty acids as a possible therapy. Nowadays, the existence of several other uterine tumors not yet well-classified, presenting uncertain malignancy and similar features both common to the benign leiomyoma and to the malignant leiomyosarcoma, let identify specific markers in order to precisely define each variant and then to pursue the correct therapy, avoiding misdiagnosis.

With this work, it has been possible to shed new light on the ability of FTIRM to characterize specific spectral signatures distinguishing benign and malignant uterine lesions, with the possibility to improve the diagnosis of intermediate and atypical variants. Moreover, the effects induced by EPA and DHA on both cell lines pave the way on further analyses to investigate their role as possible treatments or as adjuvant therapies.

CRediT authorship contribution statement

Conceptualization PC, EG; Data curation AB, VN; Formal analysis AB, SG, VN; Investigation AB, SG, VN, PP; Methodology EG, PC; Project administration PC, EG; Resources EG, PC; Software AB, VN; Supervision EG, PC; Validation AB, SG, VN; Visualization VN, EG, PC; Roles/Writing - original draft AB, SG; Writing - review & editing AB, SG, VN, PP, EG, PC.

Funding

This research did not receive any specific grant from funding agencies in the public, commercial, or not-for-profit sectors.

Declaration of competing interest

The authors declare that they have no known competing financial interests or personal relationships that could have appeared to influence the work reported in this paper.

Data availability

Data will be made available on request.

References

[1] L.R.C. Ledford, S. Lockwood, Scope and epidemiology of gynecologic cancers: an overview, Semin. Oncol. Nurs. 35 (2019) 147–150, https://doi.org/10.1016/j.soncn.2019.03.002.

[2] Q. Yang, M. Ciebiera, M.V. Bariani, M. Ali, H. Elkafas, T.G. Boyer, A. Al-Hendy, Comprehensive Review of Uterine Fibroids: Developmental Origin, Pathogenesis, and Treatment, 2022, https://doi.org/10.1210/endrev/bnab039.

[3] M.S. Islam, O. Protic, S.R. Giannubilo, P. Toti, A.L. Tranquilli, F. Petraglia, M. Castellucci, P. Ciarmela, Uterine leiomyoma: available medical treatments and new possible therapeutic options, J. Clin. Endocrinol. Metab. 98 (2013) 921–934, https://doi.org/10.1210/jc.2012-3237.

[4] K. Kodama, K. Sonoda, M. Kijima, S. Yamaguchi, H. Yagi, M. Yasunaga, T. Ohgami, I. Onoyama, E. Kaneki, K. Okugawa, H. Yahata, Y. Ohishi, Y. Oda, K. Kato, Retrospective analysis of treatment and prognosis for uterine leiomyosarcoma: 10-year experience of a single institute, Asia Pac. J. Clin. Oncol. 16 (2020) e63–e67, https://doi.org/10.1111/ajco.13286.

[5] H. Asano, T. Isoe, Y.M. Ito, N. Nishimoto, Y. Watanabe, S. Yokoshiki, Status of the Current Treatment Options and Potential Future Targets in Uterine Leiomyosarcoma: A Review, 2022, pp. 1–13.

[6] S.Ö. Özkara, Attila, uterine smooth muscle tumors: a review, MAS J. Appl. Sci. 7 (2022) 291–298, https://doi.org/10.52520/masjaps.v7i2id172.

[7] E.A. Pritts, W.H. Parker, J. Brown, D.L. Olive, Outcome of occult uterine leiomyosarcoma after surgery for presumed uterine fibroids: a systematic review, J. Minim. Invasive Gynecol. 22 (2015) 26–33, https://doi.org/10.1016/j.jmig.2014.08.781.

[8] C.L. Adams, I. Dimitrova, M.D. Post, L. Gibson, M.A. Spillman, K. Behbakht, A. P. Bradford, Identification of a novel diagnostic gene expression signature to discriminate uterine leiomyoma from leiomyosarcoma, Exp. Mol. Pathol. 110 (2019), 104284, https://doi.org/10.1016/j.yexmp.2019.104284.

[9] A. Mas, C. Simón, Molecular differential diagnosis of uterine leiomyomas and leiomyosarcomas, Biol. Reprod. 101 (2019) 1115–1123, https://doi.org/10.1093/biolre/ioy195.

[10] J.Y. Cui, R. Rosa, Jason D. Wright, Hou, Uterine leiomyosarcoma: a review of recent advances in molecular biology, clinical management and outcome, An Int. J. Obstet. Gynaecol. 38 (2017) 42–49, https://doi.org/10.1111/1471-0528.14579.

[11] P.P.C. Ip, K.Y. Tse, K.F. Tam, Uterine smooth muscle tumors other than the ordinary leiomyomas and leiomyosarcomas: a review of selected variants with emphasis on recent advances and unusual morphology that may cause concern for malignancy, Adv. Anat. Pathol. 17 (2010) 91–112, https://doi.org/10.1097/PAP.0b013e3181cfb901.

[12] A. Gadducci, G.F. Zannoni, Uterine smooth muscle tumors of unknown malignant potential: a challenging question, Gynecol. Oncol. 154 (2019) 631–637, https://doi.org/10.1016/j.ygyno.2019.07.002.

[13] F. Borella, S. Cosma, D. Ferraioli, I. Ray-Coquard, N. Chopin, P. Meeus, V. Cockenpot, G. Valabrega, G. Scotto, M. Turinetto, N. Biglia, L. Fuso, L. Mariani, D. Franchi, A.M. Vidal Urbinati, I. Pino, G. Bertschy, M. Preti, C. Benedetto, I. Castellano, P. Cassoni, L. Bertero, Clinical and histopathological predictors of recurrence in uterine smooth muscle tumor of uncertain malignant potential (STUMP): a multicenter retrospective cohort study of tertiary centers, Ann. Surg. Oncol. 29 (2022) 8302–8314, https://doi.org/10.1245/s10434-022-12353-y.

[14] J. Di Giuseppe, C. Grelloni, L. Giuliani, G.D. Carpini, L. Giannella, A. Ciavattini, Recurrence of uterine smooth muscle tumor of uncertain malignant potential: a systematic review of the literature, Cancers (Basel). 14 (2022), https://doi.org/10.3390/cancers14092323.

[15] P. Saldeen, T. Saldeen, Women and omega-3 fatty acids, Obstet. Gynecol. Surv. 59 (2004) 722–730, https://doi.org/10.1097/01.ogx.0000140038.70473.96.

[16] P.C. Calder, Omega-3 fatty acids and inflammatory processes, Nutrients. 2 (2010) 355–374, https://doi.org/10.3390/nu2030355.

[17] D. Swanson, R. Block, S.A. Mousa, Omega-3 fatty acids EPA and DHA: health benefits throughout life, Am. Soc. Nutr. 3 (2012) 1–7, https://doi.org/10.3945/an.111.000893.

[18] M.W.-W. Bianka Bojková, Pawel J. Winklewski, Dietary fat and cancer — which is good, which is bad, and the body of evidence, Int. J. Mol. Sci. - MDPI. 21 (2020), https://doi.org/10.3390/ijms21114114.

[19] M.B. Covington, Omega-3 fatty acids, Am. Fam. Physician - Complement. Altern. Med. 70 (2004) 133–140.

[20] W.S. Harris, Omega-3 fatty acids, Encycl. Diet. (Suppl) (2004) 493–504, https://doi.org/10.1081/E-EDS-120022075.

[21] R. Gorjão, A.K. Azevedo-martins, H. Gomes, F. Abdulkader, M. Arcisio-miranda, J. Procopio, R. Curi, Comparative effects of DHA and EPA on cell function, Pharmacol. Ther. 122 (2009) 56–64, https://doi.org/10.1016/j.pharmthera.2009.01.004.

[22] M. Busacca, M.E.C. Massimo Candiani, D. Vito Chiàntera, A.D.G. Cristofaro, S. G. Stefano, L. Caterina Exacoustos, M.M. Stefano Lazzeri, S. Luisi, V.R. Micalef, R. Fabio Parazzini, F. Seracchioli, M. Sorbi, F.P. Vignali, Errico Zupi, Guidelines for diagnosis and treatment of endometriosis, Ital. J. Gynaecol. Obstet. 30 (2018), https://doi.org/10.14660/2385-0868-85.

[23] M. Ali, R. Haque, S.A. Khan, Docosahexaenoic Acid (DHA): A Dietary Supplement With Promising Anticancer Potential, Elsevier Inc., 2019, https://doi.org/10.1016/B978-0-12-811297-7.00030-5.

[24] M. Ciebiera, S. Esfandyari, H. Siblini, L. Prince, H. Elkafas, C. Wojtyła, A. Al-hendy, M. Ali, Nutrition in Gynecological Diseases: Current Perspectives, 2021, pp. 1–33.

[25] K.Y. Yoshihiko Mano, Ayaka Kato, Nobuo Fukuda, Keiko Yamada, Influence of Ingestion of Eicosapentaenoic Acid-rich Fish Oil on Oxidative Stress at the Menstrual Phase: A Randomized, Double-blind, Placebo-controlled, Parallel-group Trial, Women's 3, 2022, pp. 643–651, https://doi.org/10.1089/whr.2022.0003.

[26] M.S. Islam, A. Ciavattini, F. Petraglia, M. Castellucci, P. Ciarmela, Extracellular matrix in uterine leiomyoma pathogenesis: a potential target for future therapeutics, Hum. Reprod. Update 24 (2018) 59–85, https://doi.org/10.1093/humupd/dmx032.

[27] A. Giuliani, S. Greco, S. Pacilè, A. Zannotti, G. Delli Carpini, G. Tromba, S. R. Giannubilo, A. Ciavattini, P. Ciarmela, Advanced 3D imaging of uterine Leiomyoma's morphology by propagation-based phase-contrast microtomography, Sci. Rep. 9 (2019) 1–11, https://doi.org/10.1038/s41598-019-47048-0.

[28] A. Belloni, M. Furlani, S. Greco, V. Notarstefano, C. Pro, B. Randazzo, P. Pellegrino, A. Zannotti, G. Delli, A. Ciavattini, F. Di, E. Giorgini, A. Giuliani, S. Cinti, P. Ciarmela, Uterine leiomyoma as useful model to unveil morphometric and macromolecular collagen state and impairment in fibrotic diseases: an ex-vivo human study, BBA - Mol. Basis Dis. 1868 (2022), 166494, https://doi.org/10.1016/j.bbadis.2022.166494.

[29] B. Burger, C.M.C. Kühl, T. Candreva, R. da S. Cardoso, J.R. Silva, B.G. Castelucci, S. R. Consonni, H.L. Fisk, P.C. Calder, M.A.R. Vinolo, H.G. Rodrigues, Oral administration of EPA-rich oil impairs collagen reorganization due to elevated production of IL-10 during skin wound healing in mice, Sci. Rep. 9 (2019) 1–13, https://doi.org/10.1038/s41598-019-45508-1.

[30] V. Notarstefano, S. Sabbatini, C. Pro, A. Belloni, L.V. Giulia Orilisi, Corrado Rubini, Hugh J. Byrne, E. Giorgini, Exploiting fourier transform infrared and Raman microspectroscopies on cancer stem cells from oral squamous cells carcinoma : new evidence of acquired cisplatin chemoresistance, Analyst. 145 (2020) 8038–8049, https://doi.org/10.1039/d0an01623c.

[31] V. Notarstefano, A. Belloni, S. Sabbatini, C. Pro, G. Orilisi, R. Monterubbianesi, V. Tosco, H.J. Byrne, L. Vaccari, E. Giorgini, Cytotoxic effects of 5-azacytidine on primary tumour cells and cancer stem cells from oral squamous cell carcinoma: an in vitro FTIRM analysis, Cells. (2021), https://doi.org/10.3390/cells10082127.

[32] V. Notarstefano, S. Sabbatini, M. Sabbatini, A. Arrais, A. Belloni, C. Pro, L. Vaccari, D. Osella, E. Giorgini, Hyperspectral characterization of the MSTO-211H cell spheroid model: a FPA–FTIR imaging approach, Clin. Spectrosc. 3 (2021), 100011, https://doi.org/10.1016/j.clispe.2021.100011.

[33] R. Campagna, A. Belloni, V. Pozzi, A. Salvucci, V. Notarstefano, L. Togni, M. Mascitti, D. Sartini, E. Giorgini, E. Salvolini, A. Santarelli, L. Lo Muzio, M. Emanuelli, Role played by paraoxonase-2 enzyme in cell viability, proliferation and sensitivity to chemotherapy of oral squamous cell carcinoma cell lines, Int. J. Mol. Sci. - MDPI. 24 (2023) 338, https://doi.org/10.3390/ijms24010338.

[34] J.S. Rhim, Generation of immortal human prostate cell lines for the study of prostate cancer, Prostate Cancer Methods Protoc. 81 (2003) 69–77, https://doi.org/10.1385/1-59259-372-0:69.

[35] M. Malik, J. Webb, W.H. Catherino, Retinoic acid treatment of human leiomyoma cells transformed the cell phenotype to one strongly resembling myometrial cells, Clin. Endocrinol. 69 (2008) 462–470, https://doi.org/10.1111/j.1365-2265.2008.03207.x.

[36] C. Petibois, G. Gouspillou, K. Wehbe, J.P. Delage, G. Déléris, Analysis of type i and IV collagens by FT-IR spectroscopy and imaging for a molecular investigation of skeletal muscle connective tissue, Anal. Bioanal. Chem. 386 (2006) 1961–1966, https://doi.org/10.1007/s00216-006-0828-0.

[37] V. Notarstefano, G. Gioacchini, H.J. Byrne, C. Zacà, E. Sereni, L. Vaccari, A. Borini, O. Carnevali, E. Giorgini, Vibrational characterization of granulosa cells from patients affected by unilateral ovarian endometriosis: new insights from infrared and Raman microspectroscopy, Spectrochim. Acta A Mol. Biomol. Spectrosc. 212 (2019) 206–214, https://doi.org/10.1016/j.saa.2018.12.054.

[38] V. Notarstefano, S. Sabbatini, C. Conti, M. Pisani, P. Astolfi, C. Pro, C. Rubini, L. Vaccari, E. Giorgini, Investigation of human pancreatic cancer tissues by Fourier Transform Infrared Hyperspectral Imaging, J. Biophotonics 13 (2020) 1–10, https://doi.org/10.1002/jbio.201960071.

[39] B. Vileno, S. Jeney, A. Sienkiewicz, P.R. Marcoux, L.M. Miller, L. Forró, Evidence of lipid peroxidation and protein phosphorylation in cells upon oxidative stress photo-generated by fullerols, Biophys. Chem. 152 (2010) 164–169, https://doi.org/10.1016/j.bpc.2010.09.004.

[40] A.C.S. Talari, M.A.G. Martinez, Z. Movasaghi, S. Rehman, I.U. Rehman, Advances in Fourier transform infrared (FTIR) spectroscopy of biological tissues, Appl. Spectrosc. Rev. 52 (2017) 456–506, https://doi.org/10.1080/05704928.2016.1230863.

[41] M. Lombó, C. Giommi, M. Paolucci, V. Notarstefano, N. Montik, G. Delli Carpini, A. Ciavattini, A. Ragusa, F. Maradonna, E. Giorgini, O. Carnevali, Preeclampsia correlates with an increase in cannabinoid receptor 1 levels leading to macromolecular alterations in chorionic villi of term placenta, Int. J. Mol. Sci. 23 (2022) 12931, https://doi.org/10.3390/ijms232112931.

[42] M. Banyay, M. Sarkar, A. Gräslund, A library of IR bands of nucleic acids in solution, Biophys. Chem. 104 (2003) 477–488, https://doi.org/10.1016/S0301-4622(03)00035-8.

[43] S.-Y. Lin, M.-J. Li, W.-T. Cheng, FT-IR and Raman vibrational microspectroscopies used for spectral biodiagnosis of human tissues, Spectroscopy. 21 (2007) 1–30.

[44] V. Notarstefano, M. Pisani, M. Bramucci, L. Quassinti, F. Maggi, L. Vaccari, M. Parlapiano, E. Giorgini, P. Astolfi, A vibrational in vitro approach to evaluate

the potential of monoolein nanoparticles as isofuranodiene carrier in MDA-MB 231 breast cancer cell line: new insights from infrared and Raman microspectroscopies, Spectrochim. Acta Part A Mol. Biomol. Spectrosc. 269 (2022), 120735, https://doi.org/10.1016/J.SAA.2021.120735.

[45] P. Zucchiatti, E. Mitri, S. Kenig, F. Bille, G. Kourousias, D.E. Bedolla, L. Vaccari, Contribution of ribonucleic acid (RNA) to the fourier transform infrared (FTIR) Spectrum of eukaryotic cells, Anal. Chem. 88 (2016) 12090–12098, https://doi.org/10.1021/acs.analchem.6b02744.

[46] D.R. Whelan, K.R. Bambery, P. Heraud, M.J. Tobin, M. Diem, D. McNaughton, B. R. Wood, Monitoring the reversible B to A-like transition of DNA in eukaryotic cells using Fourier transform infrared spectroscopy, Nucleic Acids Res. 39 (2011) 5439–5448, https://doi.org/10.1093/nar/gkr175.

[47] G.I. Dovbeshko, V.I. Chegel, N.Y. Gridina, O.P. Repnytska, Y.M. Shirshov, V. P. Tryndiak, I.M. Todor, G.I. Solyanik, Surface enhanced IR absorption of nucleic acids from tumor cells: FTIR reflectance study, Biopolymers. 67 (2002) 470–486, https://doi.org/10.1002/bip.10165.

[48] M. Flynn, M. Jamison, S. Datta, E. Myers, Health care resource use for uterine fibroid tumors in the United States, Am. J. Obstet. Gynecol. 195 (2006) 955–964, https://doi.org/10.1016/j.ajog.2006.02.020.

[49] E. Giuliani, S. As-Sanie, E.E. Marsh, Epidemiology and management of uterine fibroids, Int. J. Gynecol. Obstet. 149 (2020) 3–9, https://doi.org/10.1002/ijgo.13102.

[50] M. Tantari, F. Barra, S. Di Domenico, D. Ferraioli, V.G. Vellone, F. De Cian, S. Ferrero, Current state of the art and emerging pharmacotherapy for uterine leiomyosarcomas, Expert. Opin. Pharmacother. 20 (2019) 713–723, https://doi.org/10.1080/14656566.2019.1571042.

[51] P.C. Calder, P. Yaqoob, Omega-3 polyunsaturated fatty acids and human health outcomes, BioFactors. 35 (2009) 266–272, https://doi.org/10.1002/biof.42.

[52] J. Chris Bradberry, D.E. Hilleman, Overview of omega-3 fatty acid therapies, P T. 38 (2013) 681–691.

[53] M.S. Islam, C. Castellucci, R. Fiorini, S. Greco, R. Gagliardi, A. Zannotti, S. R. Giannubilo, A. Ciavattini, N.G. Frega, D. Pacetti, P. Ciarmela, Omega-3 fatty acids modulate the lipid profile, membrane architecture, and gene expression of leiomyoma cells, J. Cell. Physiol. 233 (2018) 7143–7156, https://doi.org/10.1002/jcp.26537.